Electron Beam-Plasma Interactions with the Versatile Toroidal Facility (VTF) for Ionospheric Simulation

by

Suzanne Marie Murphy

S.B., Electrical Engineering, M.I.T. (1994)

Submitted to the Department of Electrical Engineering and Computer Science
in partial fulfillment of the requirements for the degree of

Master of Engineering in Electrical Engineering and Computer Science

at the

MASSACHUSETTS INSTITUTE OF TECHNOLOGY

September 1995
[February 1996]

Author .....
Department of Electrical Engineering and Computer Science
August 11, 1995

Certified by .....
Professor Min-Chang Lee
Thesis Supervisor

Accepted by .....
Frederic R. Morgenthaler
Chairman, Department Committee on Graduate Theses

Electron Beam-Plasma Interactions with the Versatile Toroidal Facility (VTF) for Ionospheric Simulation

by

Suzanne Marie Murphy

Submitted to the Department of Electrical Engineering and Computer Science
on August 11, 1995, in partial fulfillment of the
requirements for the degree of
Master of Engineering in Electrical Engineering and Computer Science

Abstract

An investigation of electron beam-plasma interactions in the laboratory is conducted to cross-check the 1992 TSS-1 space shuttle experiments. Because active experiments in space plasmas are often expensive and difficult to conduct on a frequent basis, there arises a need for laboratory simulations. The Versatile Toroidal Facility (VTF) at the MIT Plasma Fusion Center has been used to generate a large magnetized plasma with overdense conditions as a method of simulating shuttle and ionospheric heating experiments. The capabilities of the Taylor discharge method as well as electron beams emitted from LaB_6 filaments are explored to provide an overdense background plasma. Electron beams are also used to represent to the electron guns in the shuttle experiments. A vertical langmuir probe is designed and built to characterize the plasma behavior in close proximity to the electron beam. A radial side probe is used to measure data at mid-plane for comparison. Limitations on the current studies are described and future work for further investigation is discussed.

Thesis Supervisor: Professor Min-Chang Lee
Title: Head, Ionospheric Plasma Research Group
MIT Plasma Fusion Center

Acknowledgments

First and foremost I would like to extend my thanks and gratitude to Professor Min-Chang Lee. He is a continual source of encouragement and enthusiasm and his dedication to research has taught me a great deal.

I would also like to thank Bill Burke, my focal point at Phillips Laboratory this past summer. He has always taken interest in my work and his sharp ideas have helped me to focus on important points relating to this project. Thanks also to David Cooke, from Phillips Laboratory, who has also given support to this project and whose conversations provided me with a better understanding of the space shuttle experiments.

I would also like to thank Ryan Riddolls and Dan Moriarty for their valuable help and advice which facilitated the planning and execution of my experiments. Thanks also to Ed Fitzgerald, Bob Childs, and several others at the Plasma Fusion Center whose help and advice aided the design and construction of my probe.

Finally, I would like to thank my family and all of my friends for their constant support and encouragement. They have been a source of strength and love which has helped me to persevere throughout my studies at M.I.T.

Contents

List of Figures

List of Tables

Chapter 1

Introduction

1.1 Overview

The Versatile Toroidal Facility (VTF) at the MIT Plasma Fusion Center has been used for several years to study wave propagation and turbulence in plasmas. Because of the many ionospheric heating and shuttle experiments there has grown a need for laboratory simulations of ionospheric conditions. VTF is capable of filling that need, specifically by simulating electron beam experiments that were conducted with the space shuttle Tethered Satellite System (TSS) in 1992. The Taylor discharge method is explored in conjunction with LaB_6 filaments to produce a steady state plasma, analogous to the background plasma in the ionosphere. An electron beam is pulsed to simulate the beam injected in the space plasmas. The results of these experiments will be compared with the data obtained in the TSS experiments to determine how well plasma turbulence generated inside the VTF can be used to study ionospheric plasmas.

1.2 Thesis Outline

This thesis is organized as follows: Chapter 2 provides background on the TSS-1 space shuttle experiments, and the VTF laboratory experiments and how they were carried out. The design of the vertical probe, along with its operation, is delineated

and the data acquisition system is described. Chapter 3 contains details on producing ionospheric conditions including the Taylor discharge method and electron beam interaction. The conditions of VTF are compared with other laboratory setups which are also being used for ionospheric simulation. Chapter 4 provides analysis of the results from the radial and vertical probes. Chapter 5 contains conclusions based on what has been accomplished. The current limitations are explained as is the need for future research in this area.

Chapter 2

Space and Laboratory Experiments

2.1 Space Shuttle Experiments

The Tethered Satellite System (TSS) was launched aboard the Space Shuttle STS-46 Atlantis which flew from July 31 to August 6, 1992, as a joint effort between the United States and Italy. Of the many experiments that were carried out on this mission, this project focuses on the Shuttle Potential and Return Electron Experiment (SPREE), which utilizes electrostatic analyzers in the shuttle payload bay to make measurements of particle energy and power spectra.

The shuttle flew at an altitude of 300 km in a 28.5° inclination orbit. SPREE consisted of two Fast Pulsed Electron Generators (FPEG) which injected a 100 mA, 1 keV electron beam at angles nearly perpendicular to the earth's magnetic field and with turn on and turn off times of approximately 100 ns. The beam electrons were emitted through an aperture of 0.56 cm radius, with a magnetically controlled divergence of 7.5°. Two electrostatic analyzers (ESA) were also located on the opposite side of the shuttle payload. These analyzers simultaneously measured ion and electron fluxes with energies from 10 eV to 10 keV and within a 100° x 8° angular fan. This angular region was divided into 10 zones of 10° width. Ion and electron spectra were measured

independently in each zone. The two analyzers, labeled A and B, were mounted on rotary tables and placed back to back on the shuttle payload. The motion of these analyzers were synchronized so that both ion and electron spectra were sampled over a solid angle of 2π steradians every 30 s. To prevent saturated measurements, the geometric factors of ESA B were set to be around 100 times smaller than those for ESA A. The energy resolution for each of the electron channels is $\triangle E/E \approx 7\%$. The arrival times of individual electrons were also measured to detect particle bunching and hence, signify resonant wave-particle interactions [Dobrowolny, 1994].

Many sources of error in the SPREE measurements had to be taken into account. The current collection may have been affected by induced localized discharges due to Orbiter outgassing, thruster actions, water dumps and the presence of neutral gas in the vicinity of the shuttle. In addition, the size of the sheath that formed around the shuttle may also have had an effect on the particle measurements. The experimental setup is more complex than the conditions laid by Langmuir for a sphere at high voltage inside an unmagnetized plasma. The TSS setup is more complex because the ionosphere is magnetized and the shuttle is moving in a meso-sonic plasma since its velocity is supersonic with respect to ions and subsonic with respect to electrons [Dobrowolny, 1994].

The TSS experiments were done in the F-region of the ionosphere which extends from 100 to 350 km. This region in altitude contains overdense plasma, which exists when the electron plasma frequency, ω_{pe}, and the electron cyclotron frequency, ω_{ce}, obey the relation

$$\omega_{pe} > \omega_{ce} \tag{2.1}$$

At the shuttle's altitude of 300 km, these frequencies lie in the following ranges: $f_{ce} = 0.7$ to 1.4 MHz and $f_{pe} = 2.8$ to 8.9 MHz. For the shuttle experiments, the electron cyclotron frequency was taken to be $f_{ce} = 0.8$ MHz [Hardy, et. al., 1995]. The ratio of these frequencies thus lies in the range $3.5 < \frac{f_{pe}}{f_{ce}} < 11.1$.

This constraint for overdense plasma can also be represented in terms of the Debye length, λ_D, which represents the thickness of the plasma sheath, and the Larmor radius, r_L, the radius of a particle's gyrating orbit in the presence of a magnetic field, B. By substituting the definitions of ω_{pe} and ω_{ce} into equation 2.1 we obtain,

$$\frac{qB}{m_e} < \sqrt{\frac{n_o e^2}{\epsilon_o m_e}} \tag{2.2}$$

In terms of λ_D and r_L this constraint can be expressed as:

$$\frac{v_\perp}{r_L} < \frac{1}{\lambda_D}\sqrt{\frac{kT_e n_o}{m_e n_e}} \tag{2.3}$$

where $v_\perp$ is the drift velocity of the particle perpendicular to the magnetic field. Manipulating this equation, we find:

$$\lambda_D < \frac{r_L}{v_\perp}\sqrt{\frac{kT_e n_o}{m_e n_e}} \tag{2.4}$$

As calculated by Hardy, et. al. (1995), in the ionosphere $\lambda_D = 2$ cm and $r_L < 3.72$ cm. Thus, if $v_\perp < 3.5 \cdot 10^5$ m/s, the Debye length will be less than the Larmor radius in overdense plasmas. The parameters describing the plasma conditions in the vicinity of the shuttle are listed in Table 2.1 in comparison with laboratory conditions.

2.2 VTF Experimental Setup and Diagnostics

The VTF is set up, as shown in Figure 2-1. The magnetic field inside the chamber is produced by 18 toroidal magnets with 4 current coils running through each for a total of 72 toroidal field coils. There are 4 vertical field coils, two running outside the top of the chamber and two outside the bottom. The current through these coils produces an upward directed magnetic field inside the chamber. For a current, I_{TF}, going through the toroidal coils, we can use Amperes law to determine the resulting toroidal magnetic field:

$$\oint B \cdot ds = \mu_o \int J \cdot da \tag{2.5}$$

$$B = \frac{\mu_o 72 I_{TF}}{2\pi r} \tag{2.6}$$

The vertical field is described by the following equation:

$$B_z = \frac{\mu_o N I a^2}{2(a^2 + z^2)^{\frac{3}{2}}} \tag{2.7}$$

where N is 4, a is sthe radius of the coils, and z is the height above the plane of the loop, at the center.

The experiments conducted in this project will utilize one of the four available filaments as well as the Taylor discharge unit which is described in the following section. Figure 2-2 shows the position of the vertical probe and the four filaments in the chamber. The filaments, are labeled: South Top, North Middle, South Bottom, and North Top. The names refer to the power supplies being used for each filament. The terms *filament voltage* and *filament current* refer to the 11 V that is applied to heat up the filament, and the resulting current, respectively. The term *arc voltage* refers to the negative bias voltage that is applied across the filament to cause electron emission. *arc current* refers to the current that is emitted after the arc voltage has been applied.

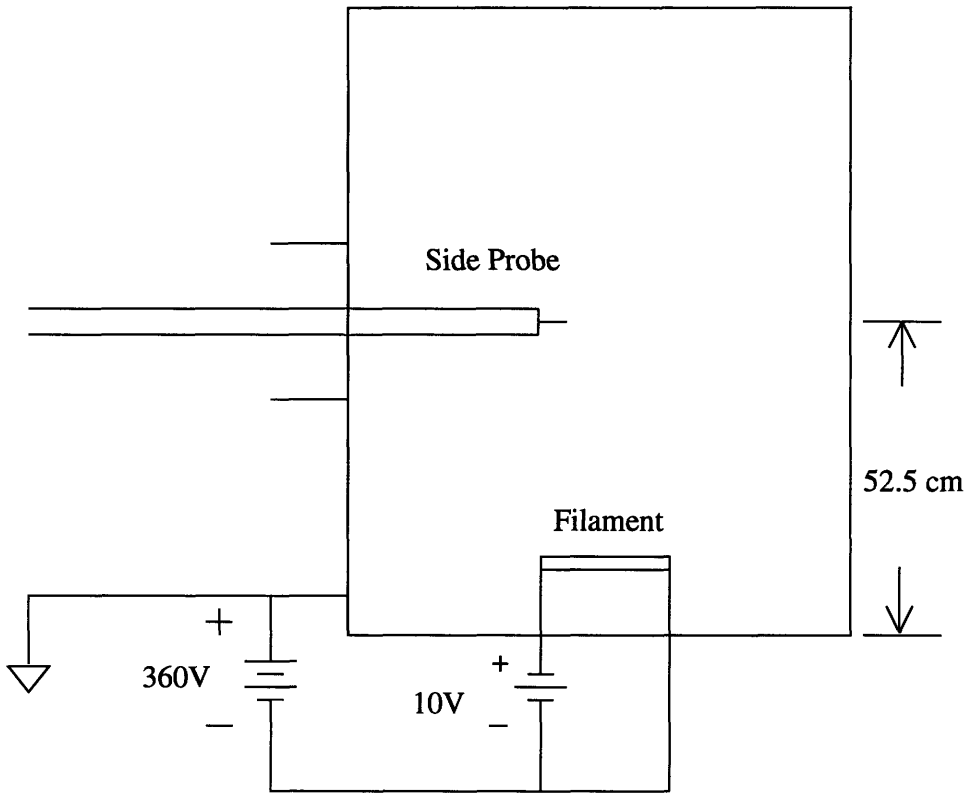

Figure 2-1: Cross Section of VTF Showing Side Probe Position.

Both Hydrogen and Argon were available to use as the neutral fill gas in VTF. However, the Argon plasmas tended to be more dense and consistent than the Hydrogen plasmas. In most of these experiments, the chamber was filled with Argon to a neutral pressure of approximately $9.8 \cdot 10^{-5}$ Torr. The number measured by the pressure meter was $7 \cdot 10^{-5}$ which is calibrated for Nitrogen pressure. The Argon pressure is obtained by multiplying by a factor of 1.4. The plasma density ranges between $8 \cdot 10^{10}$ cm^{-3} for Taylor discharge to 10^{12} cm^{-3} for beam plasmas.

As a result of upper hybrid calibration it has been found that Argon ions are multiply ionized in this plasma. When a 3 kW RF signal at 2.45 GHz was injected into the machine, the electron cyclotron frequency at the position of peak density was found to be $f_{ce} = 2.1\ GHz$. Using the upper hybrid resonance formula:

$$f_{uh}^2 = f_{pe}^2 + f_{ce}^2 \tag{2.8}$$

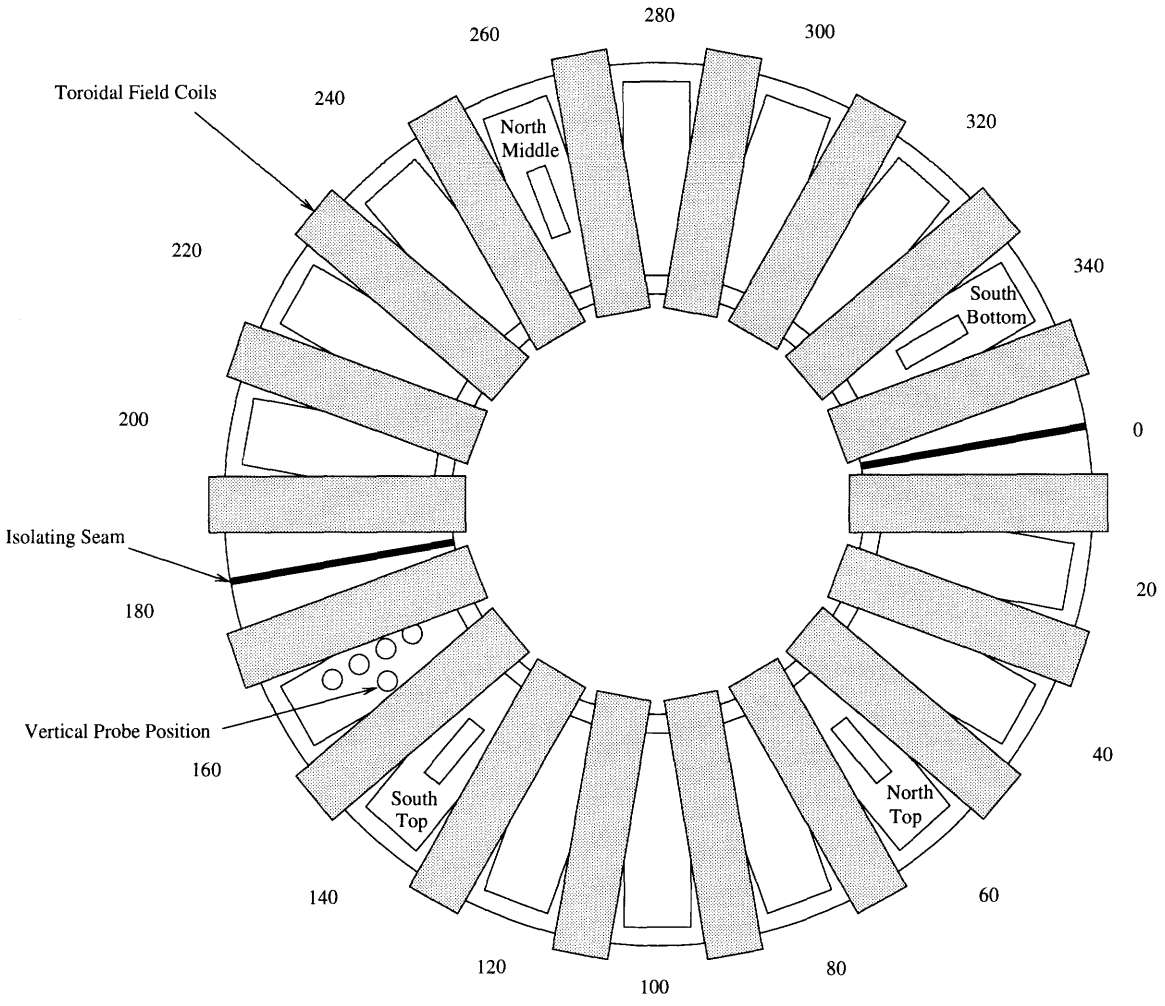

Figure 2-2: Map of the VTF Chamber Floor Including Positions of Vertical Probe and the Four Filaments: South Top, North Middle, South Bottom, and North Top. (Drawing Not to Scale)

Table 2.1: Table of Parameters for Shuttle and VTF.

	VTF	Space Shuttle
Background Density (cm^{-3})	0	10^4
Beam Density (cm^{-3})	10^{12}	1 to $5{\cdot}10^4$
Acceleration Potential (V)	360	1000
Neutral Pressure (T)	$9.8 \cdot 10^{-5}$	10^{-6}
Magnetic Field (G)	1200-1800	0.3

we find that $f_{pe1} = 1.26\ GHz$ when $f_o = 2.45\ GHz$. However, with a measured density of $5.5 \cdot 10^{10}$ cm^{-3} and assuming single ionization, we get $f_{pe2} = 2.11\ GHz$. The ratio of the corresponding densities is $\frac{n_2}{n_1} = \left(\frac{f_{pe2}}{f_{pe1}}\right)^2 = 2.8$, which indicates that the plasma exhibits double and triple ionization.

2.2.1 Langmuir Probe Operation

Two Langmuir probes were used to make measurements in the VTF. The first is a side probe which sweeps across the radius of the chamber. The tip of this probe consists of a flat, square piece of copper, 0.63 cm on each side, for a cross-sectional area of 0.40 cm^2. The tip is oriented such that the flat surface is normal to the beam direction. The other probe is a vertical probe, placed at the bottom of the chamber. The design of this probe is further explained in section 2.2.2.

The first experiments performed with the radial probe consisted of density measurements. The Langmuir probe was swept across the radius from the inner wall to the outer wall. The probe was negatively biased to -100 V using a power supply. In this way the ion saturation current is measured, which can be used to calculate plasma density in the vicinity of the probe. The I-V characteristics of a Langmuir probe are described in detail by Hutchinson (1987). He derives the current measured by a Langmuir probe to be:

$$I = n_\infty e A_p \sqrt{\frac{T_e}{m_i}} \left[\frac{1}{2}\sqrt{\frac{2m_i}{\pi m_e}} exp\left(\frac{e(V_o - V_f)}{T_e}\right) - \frac{A_s}{A_p} exp\left(-\frac{1}{2}\right)\right] \qquad (2.9)$$

where n_∞ is the density at steady-state, $V_\circ$ is the probe potential, A_s is the area of the sheath, and A_p is the area of the probe. When the probe is biased to a voltage much lower than the floating potential, V_f, the electron current is negligible, and the ion saturation current density is found to be:

$$J_i = n_\infty e \, exp\left(-\frac{1}{2}\right)\sqrt{\frac{T_e}{m_i}} \tag{2.10}$$

It should be recognized that the equation for ion saturation current is derived for the case of an unmagnetized plasma, however most of the current being measured is traveling parallel to the magnetic field so this formula will be adequate. We then find the current by multiplying by the projected area of the Langmuir probe tip, A_p, seen by this current.

$$I_s = J_i A_p \tag{2.11}$$

If we know the electron temperature, in eV, then the current measurement can be used to find n_∞, the steady-state plasma density:

$$n_\infty = \frac{I_s}{eA_p} exp\left(\frac{1}{2}\right)\sqrt{\frac{M_i}{T_e}} \tag{2.12}$$

As mentioned earlier, the area of the side probe is A_p =0.4 cm^2. The area of the vertical probe tip seen by an approaching beam is 0.63 cm by 0.0625 cm which is equal to $3.9 \cdot 10^{-2}$ cm^2.

2.2.2 Design and Operation of a Vertical Probe

A vertical Langmuir probe was designed, built and installed on the bottom of the chamber as illustrated in Figure 2-3. This probe was positioned as close to the electron beam as possible to characterize the plasma right after the electrons are emitted from the filament. The VTF LaB_6 filaments emit electrons which are then accelerated by the applied 360 V which produces an electric field in the chamber. The velocity of electrons coming off the filament is initially zero and then increases until they hit the collector plate at the top of the machine.

A more detailed diagram of the vertical probe is shown in Figure 2-4. A flexible bellows allows the height of the probe to be adjusted easily. The bellows has 47.5 cm of throw which allows the probe to be inserted to a height of 38.1 cm above the chamber floor. A 6.25 cm hollow steel tube is welded to a blank flange and sticks into the outside end of the bellows. A piece of coaxial cable with a 0.22 cm outer diameter and a 0.063 cm inner diameter goes through a hollow ceramic tube. The length of the coax within the ceramic can be adjusted using a Cajon sliding seal with a 0.156 cm diameter. The seal is mounted on the end of the probe assembly.

The three different versions of this vertical probe are shown in Figure 2-5. In the first installation, this steel tube was used as an anchor to hold a 60 cm ceramic tube with a 0.475 cm outer diameter. The ceramic was put inside the steel tube and a notch was cut in each tube with a stiff wire wrapped around the notch to hold the ceramic in place. The inner conductor was positioned to stick out 2 cm above the ceramic end.

In the first two installations of this probe certain setbacks occurred. When the first probe was moved directly in front of the beam path, the end of the ceramic tube melted, possibly due to a crack in the ceramic, and resulted in the outer conductor of the coax being exposed. This caused substantial arcing because the outer conductor is connected to the machine ground and thus shorts out the electron beam emitters.

In the second installation, a wider piece of ceramic was used with an outer diameter of 0.94 cm. This ceramic was placed over the steel tube and it rested on the blank flange that the steel tube is welded to. A small ceramic cap, 0.45 cm long with a 0.65 cm diameter and four small holes going through, was placed on the plasma end of the ceramic. The cap rested on the outer conductor of the coax, with the inner conductor extending through one of the four holes in the cap. The inner conductor was then bent across to the edge of the cap to keep it from sliding off. The effective length of the inner conductor sticking into the plasma was 1.3 cm. The purpose of the thicker ceramic along with the cap was to provide better shielding and prevent the electron

beam from arcing to the outer conductor of the coax which is at the same ground potential as the chamber wall. This piece of ceramic was shorter, so that the tip of the probe could only go as far as 34.4 cm above the floor of the chamber. However, when the tip was moved in front of the beam path the arcing occurred again and the end of the large ceramic melted from the heat of the outer conductor.

In the third installation, a smaller diameter ceramic tube was used. This 0.63 cm diameter ceramic has a rounded end which has a small CO_2 laser-cut hole for the inner conductor of the coax to go through. This apparatus provides the best form of shielding since the laser hole is only slightly larger than the diameter of the inner conductor, and it is the only path the current can take to reach the outer conductor. The ceramic diameter is nearly the same as that of the steel tube, so it cannot fit inside or around the steel tube. Instead, the ceramic rests on top of the steel. An aluminum collar was built and slid over the ceramic so that it is overlapping both pieces. Set screws are used to hold the ceramic and steel in place. At full retraction, the probe tip lies 11.25 cm below the chamber floor. The ceramic tube was slid over the coax so that the tip of the inner conductor sticks out with 0.63 cm exposed to the plasma. In this way, the outer conductor of the coax is well shielded from the -360 V across the filament. The data which was obtained using the different implementations are labeled *probe 1, probe 2,* and *probe 3.*

2.2.3 Data Acquisition System

Many signals were measured using the current system, including probe signals and diagnostic signals taken to monitor the beam and power supply performance. The block diagram in Figure 2-6 shows the organization of the data acquisition, as well as the Paragon process control system that is used to send instructions to the power supplies and diagnostics by way of a Programmable Logic Controller (PLC). The filament and arc voltage measurements are taken by two pairs of sense leads at the port cover of the corresponding filament. The arc and filament current measurements are taken using shunt resistors inside the power supplies. These measurements are

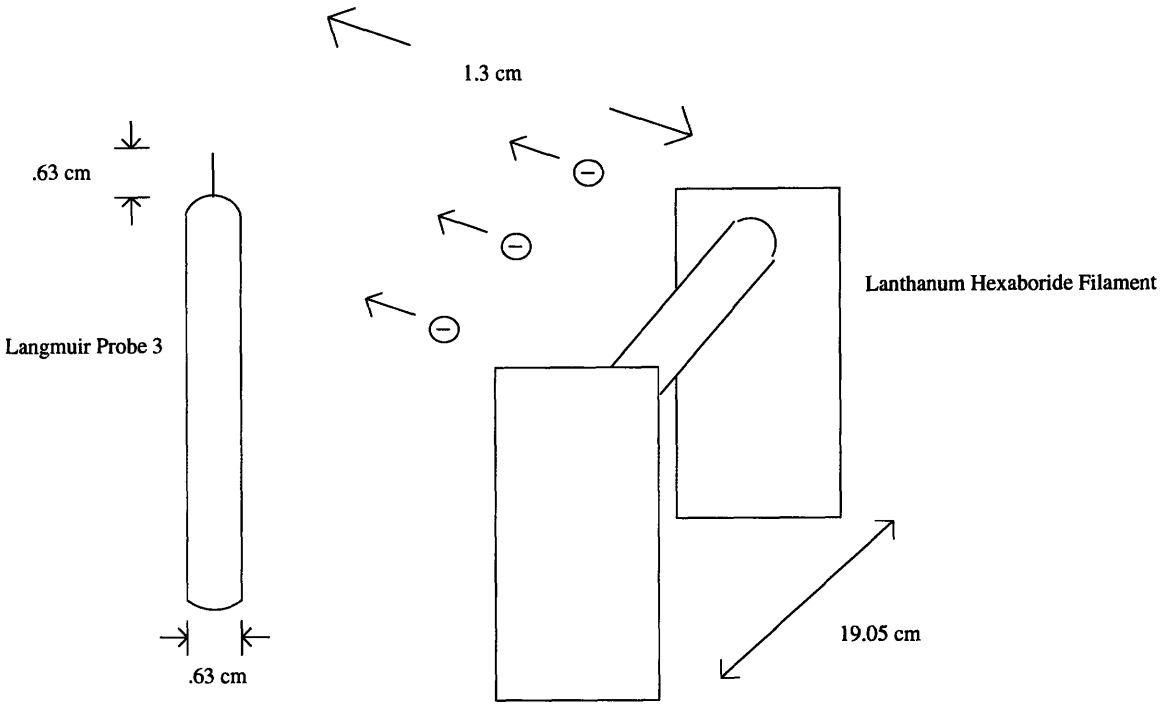

Figure 2-3: Positioning of Probe and Filament

taken at the power supply on the lower level of the cell and are fed through fiber optic transmitters to isolate the power supply ground from the digitizers. The fiber optic signals are sent upstairs to a diagnostics cabinet where they are converted back to voltage signals and then fed into a CAMAC crate which contains three LeCroy 8212 digitizers, three LeCroy 2264 digitizers, nine 48 kilobyte memory modules and two 32 kilobyte memory modules. The triggering of these digitizers is controlled by a Jorway module and a TTL 221 buffer. The CAMAC crate is remotely controlled via fiber optic connections by a data acquisition program, which is run on a PC in the control room.

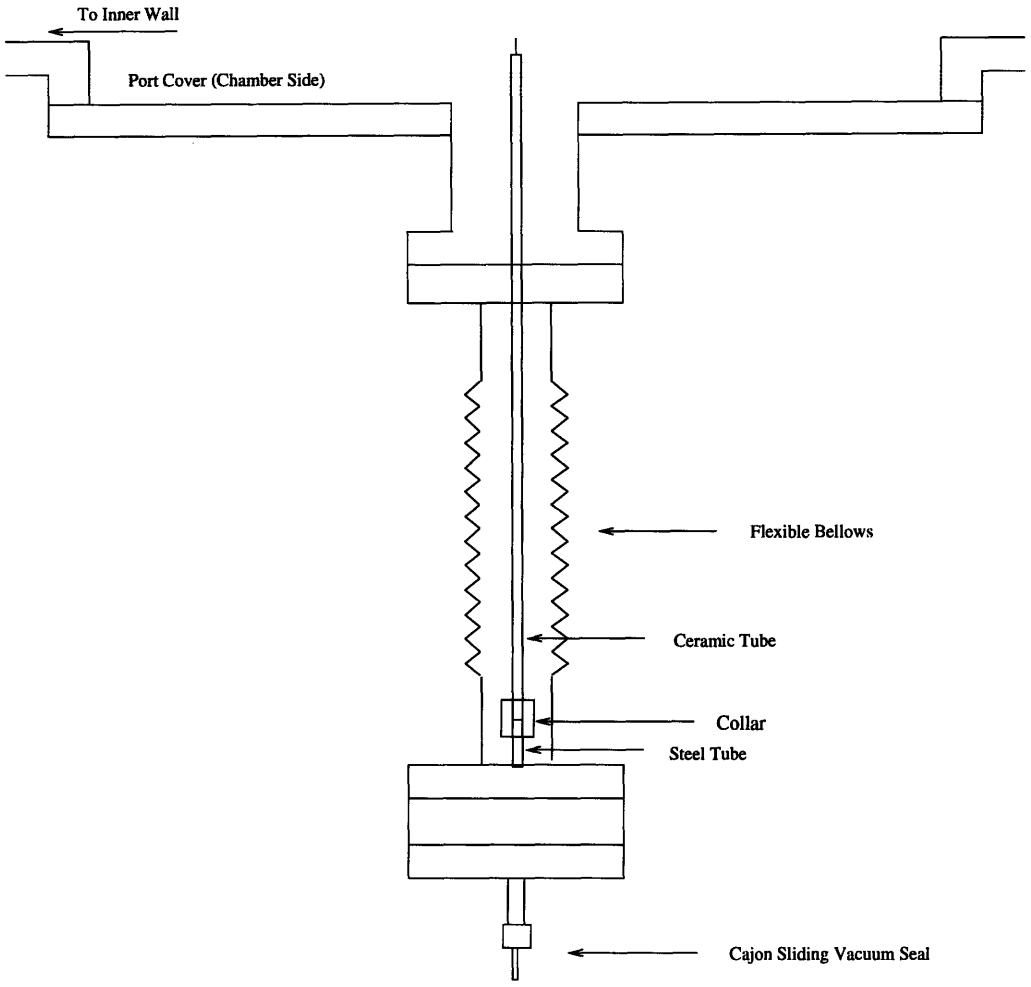

Figure 2-4: Design and Placement of Vertical Probe

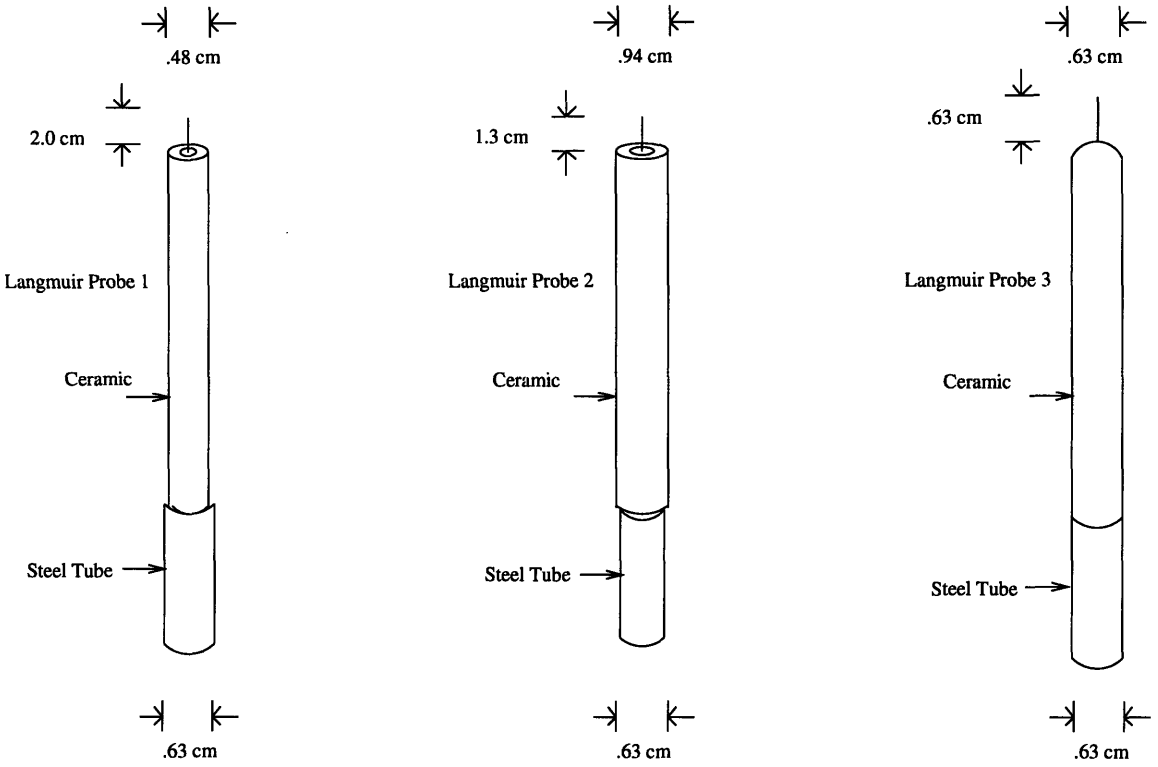

Figure 2-5: Three different Implementations of the Vertical Probe

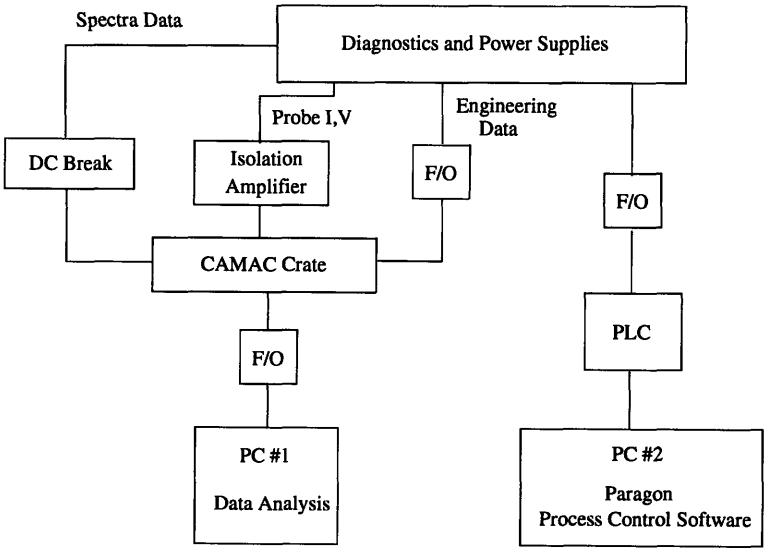

Figure 2-6: Data Acquisition and Process Control Systems for VTF

Chapter 3

Simulation of Ionospheric Conditions

3.1 Taylor Discharge Method

It has been found that a resonant LC circuit can be used to generate a plasma. This scheme for producing inductive-drive plasmas is known as Taylor discharge, developed by Robert Taylor, now at UCLA. With this method a plasma can be formed in a toroidal machine without using high voltage power supplies. The scheme involves hooking up the inner transformer coil of the chamber in series with a large capacitor and then driving the resulting LC circuit near resonance. The large reactive AC current in the inner transformer coil induces current in the plasma, which transfers energy via ohmic heating.

Finding the exact resonant frequency has proven to be difficult. Before any plasma has formed, the only load in this two-transformer model is the inductance of the secondary coil. When the plasma forms, the impedance of the load cannot be expressed as a linear expression. In general, the resistive part of the plasma load is inversely proportional to density, which causes the resistance to decrease as the plasma is formed. We also know that the density is proportional to the power that is transferred to the plasma. By substituting into the expression relating coil voltage and current, $V = IR$,

we find that the voltage across the coils is constant, which makes the modeling of this system difficult.

The Taylor discharge circuit in the VTF, constructed by Ryan Riddolls, uses one power supply that can provide up to 40 kW of DC current at 360 V [Beals, 1994]. In order to use the power supply to drive the LC circuit near resonance, the DC power from the supply must be chopped to AC power near the LC resonant frequency and coupled to the resonant circuit to achieve a high coil voltage.

The method used to achieve this DC to AC conversion is somewhat similar to the series resonant converter. The 45-turn inner transformer coil is tapped at its first and ninth turn as illustrated in Figure 3-1. A full-bridge inverter is then attached across these taps to create a square voltage waveform from the DC power. This square wave then couples into the remaining 37 turns of the transformer coil through the air core. The higher harmonics of the square wave are attenuated by the narrow-peaked transfer function of the LC circuit. When the amplitude of the sinusoidal voltage waveform across the full 45 turns of the inner transformer coil is high enough the loop voltage amplitude around the chamber reaches the breakdown voltage of the fill gas in the vacuum chamber and the plasma is formed.

We should note that when the Taylor discharge device is being run at $\approx$ 1 kHz, the millisecond confinement time of the VTF machine ensures that the plasma is extinguished during the part of the AC cycle when the loop voltage is below the breakdown voltage. If one were to change the resonant frequency, for example, by decreasing the size of the capacitor in the LC circuit, then the plasma would become continuous as the time for one period of the AC cycle became much less than the confinement time of the VTF plasma.

One major concern with respect to toroidal-shaped plasma confinement machines is that the driving of large currents through the plasma might create a distortion of the toroidal magnetic field geometry. The kink safety criterion is a rough assessment

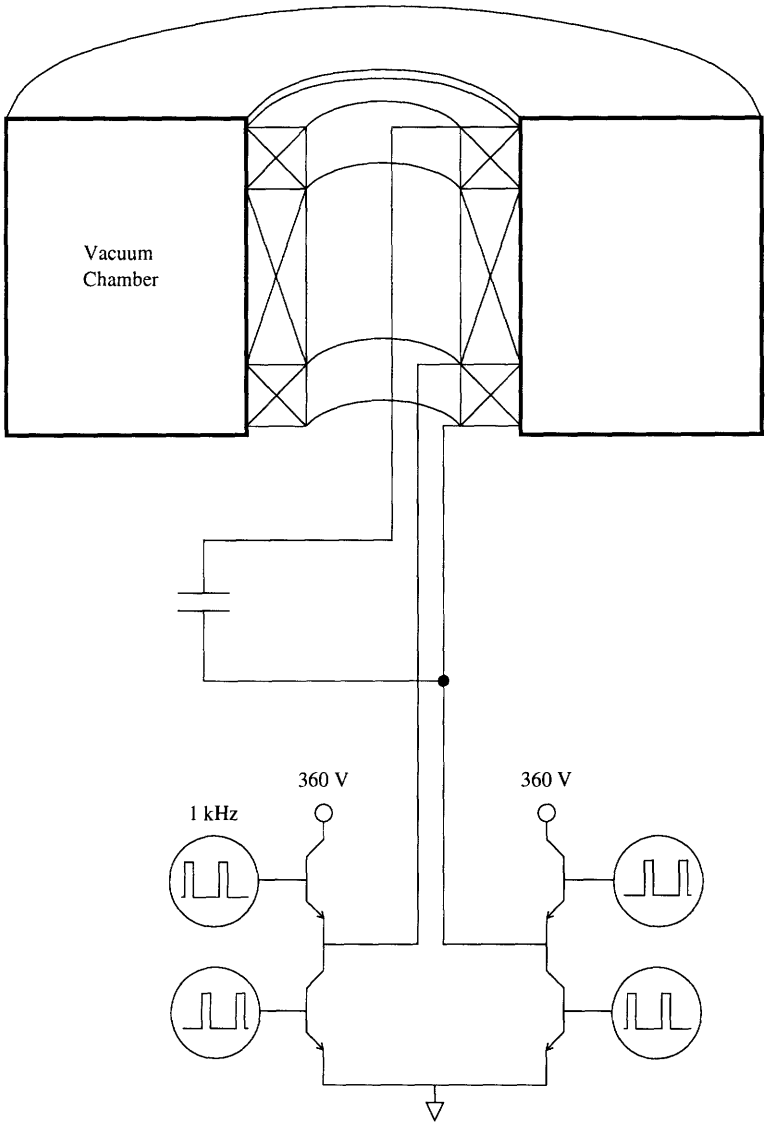

Taylor Discharge Apparatus

Figure 3-1: Taylor Discharge Setup in VTF

of this type of distortion. The criterion defines a quantity $q(r)$ and specifies the minimum value of this term such that a kink instability will not occur in a helical plasma:

$$q(r) = \frac{rB_\phi}{RB_\theta} \simeq 1 \tag{3.1}$$

where B_ϕ is the toroidal field, B_θ is the poloidal field created by the current in the plasma, R is the major radius of the toroidal plasma, and r is the radius of the assumed circular cross section of the plasma.

We recall Ampere's law for a toroidal field geometry:

$$B_\theta = \frac{\mu_0 \int J \cdot da}{2\pi r}.$$

Assuming uniform current density over the circular area of integration, B_θ reduces to

$$B_\theta = \frac{\mu_0 J r}{2} \tag{3.2}$$

and $q(r)$ becomes a constant with respect to r:

$$q_0 = \frac{2B_\phi}{\mu_0 R J} \tag{3.3}$$

The major radius, R, is equal to 92 cm and the toroidal field is 0.08 T. J is then calculated to be $1.38 \cdot 10^5 \frac{A}{m^2}$.

Now we assume a 0.5 m^2 plasma cross-sectional area, and we will continue to assume that the current density is uniformly distributed as we did in the calculation of maximum current density above. Thus the maximum current flowing in the Taylor discharge plasma without a kink instability occurring is $I_{max} = 68.6$ kA.

The BJT switches in the power supply are only rated at 300 A. This value reflected through a 45:1 ideal transformer corresponds to only 13.5 kA of plasma current. In addition, the coupling with the plasma is through an air core transformer which leads

to significant magnetizing current. These two considerations lead us to conclude that the Taylor discharge implementation on VTF cannot induce a plasma current sufficient to distort the toroidal field geometry much less induce a kink instability.

First attempts at Taylor discharge plasmas in VTF were aimed at creating overdense plasma conditions for microwave injection experiments to investigate phenomena observed in ionospheric heating experiments. While the overdense plasma condition was achieved, the density was much lower than what was envisioned at the outset of activating the Taylor discharge device. An indication of why the Taylor discharge has not performed to expectations is the low coupling of power from the supply to the plasma through two air core transformer connections, i.e. from the power supply to the 45 turn coil and from the coil to the plasma. Possible solutions include eliminating the supply to LC circuit air core transformer connection by putting the power supply directly in series with the resonant circuit, and secondly, improving the coupling of the LC circuit to the plasma by insertion of an iron core into the inner cylinder.

3.2 Beam-Plasma Interaction in VTF

To obtain an overdense plasma in the VTF we will be implementing the Taylor Discharge method as described in the previous section. We can now determine the parameters in the Taylor Discharge unit necessary to simulate the plasma conditions during the TSS shuttle mission. Previously, it has been found that the toroidal field must be at least 800 G before the density becomes independent of the field strength [Beals, 1994]. Using the formula for the electron cyclotron frequency,

$$\omega_{ce} = \frac{qB}{m_e} \tag{3.4}$$

we obtain

$$f_{ce} = \frac{\omega_{ce}}{2\pi} = 2.24GHz \tag{3.5}$$

The plasma conditions during the TSS mission demonstrate that $\frac{\omega_{pe}}{\omega_{ce}} \approx 3$. To match this condition in the VTF we need:

$$f_{pe} = \frac{\omega_{pe}}{2\pi} = 6.71\, GHz$$

Using the formula for plasma frequency,

$$\omega_{pe} = \sqrt{\frac{n_o e^2}{\epsilon_o m_e}} \tag{3.6}$$

we calculate the minimum necessary density to be:

$$n_o = 5.57 \cdot 10^{11} cm^{-3}$$

Higher density plasmas can be obtained using LaB_6 filaments which generate electron beam plasmas through thermionic emissions. When a filament is negatively biased, it emits electrons that travel upward inside the vessel. As these electrons collide with neutral particles a plasma is formed along the helical magnetic field in the VTF. One important concept related to thermionic emission is the work function. There are surface restraints that prevent most of the free electrons in a metal from leaving. These are the electrostatic forces produced by the charges in the atoms of the metal. A free electron must have a minimum kinetic energy to free itself from these forces. The work function is the work per unit charge required to free an electron from the influence of the charges in the metal. The emission equation is defined as follows:

$$J = AT^2 e^{\frac{-b_o}{T}} \tag{3.7}$$

where

$$A = 120.4\, \frac{Amp}{cm^2 K^2}$$

$$b_o = 11600 \phi_o\, K$$

and ϕ_o is the work function.

One important consideration is the Schottky Effect which occurs when the emitting surface is subjected to a positive potential gradient. The applied field effectively reduces the work function. We are then left with a constant gradient as well as the normal potential barrier. These two forces produce a new potential barrier which has a maximum at $d_c = \frac{1}{2}\sqrt{\frac{e}{4\pi\epsilon_o E}}$, the critical escape distance. After an electron exceeds d_c, the electrostatic forces are outward so the electron keeps moving and is accelerated toward the collector plate. The work function is effectively reduced by $\sqrt{\frac{eE}{4\pi\epsilon_o}}$. Half of this reduction is due to the image force being overcome, whereas the other half is due to the potential at d_c being reduced by the quantity, $d_c E$. Factors that may inhibit emission include when the free metal has been exhausted, when oxygen is present with a pressure, $P > 10^{-4}$ T, and also when $P > 10^{-3}$ T [Gewartowski, 1968].

When the two FPEGs injected electrons into the ionosphere it resulted in high energy electrons superimposed on the background maxwellian velocity distribution. Similarly, the Taylor Discharge unit on the VTF will produce a drifting maxwellian velocity distribution in the laboratory plasma. The short-pulsed electron beam emits higher energy electrons which form high velocity tail electrons. Presently, the electron beam can run with pulses as short as 10 ms. The slow turn on time of the emitter limits how fast we can pulse this beam. However, this pulse length is within the range of pulses used in the TSS experiments, which use 25 ms, 3.3 ms, and 51 μs. Because the waves can only grow as quickly as the plasma can be formed, the plasma is essentially always in steady state. But as described by Kellogg, et. al. (1986), the transient waves excited by electron beam pulses only exist for a few milliseconds of the pulse. Thus, our pulsed electron beams in conjunction with a Taylor discharge plasma, will adequately simulate the conditions observed in the ionospheric experiments for the steady state part of the FPEG pulses.

Unlike the FPEGs, the LaB_6 filaments in the VTF are not true electron guns. Rather, through thermionic emission the electrons are excited to the outer surface of the filament. Then an electric field is applied such that the electrons are repelled

and accelerated along the helical magnetic field to a collecting plate at the top of the chamber.

The path of electrons through the chamber causes ionization of the ambient neutral atoms. Because the electrons have a higher average energy, the velocity distribution becomes a drifting maxwellian in the vicinity of the beam path. Many of the electrons travel the entire way to the top of the chamber, but some diffusion also occurs out of the main stream to the chamber walls.

In order to simulate the conditions near the shuttle, it is necessary to obtain a maxwellian velocity distribution. There are presently two methods to accomplish this. The first is Electron Cyclotron Resonance Heating (ECRH). A microwave source injects 2.45 GHz O-mode waves at 3 kW of power. The waves are injected through a waveguide in the TE_{10} configuration. As the waves interact with the plasma they produce upper hybrid waves, propagating at the injected frequency, i.e., $f_{uh} = 2.45$ GHz. The conditions of the plasma in the vicinity of these waves are described by the following relation,

$$f_{uh}^2 = f_{ce}^2 + f_{pe}^2 \tag{3.8}$$

The injected microwaves excite the ambient electrons and cause ionization. Ions are considered to be cold in this case since only electrons are energized.

The densities of ECRH hydrogen plasmas produced in the VTF are typically $3 \cdot 10^{10}$ cm^{-3}, which leads to $f_{pe} \approx 9\sqrt{n} = 1.56$ GHz. Substitution of f_{pe} into equation refeq:uh gives $f_{ce} = 1.89GHz$. The ratio of the two frequencies is thus $\frac{f_{pe}}{f_{ce}} = .82$, which does not satisfy the overdense condition.

An electron beam is characterized by a small group of electrons moving in a parallel stream with velocity, v_o, and thermal velocity, v_{Te}, where $v_o \gg v_{Te}$. This system can become unstable with the excitation of plasma oscillations. The region of the distribution with positive slope can result in inverse Landau damping and unstable

wave growth. It has been shown that the electrons emitted from an energetic beam produce a bump in the velocity distribution. However, as the plasma reaches a stable state, this bump flattens out into a plateau.

This situation is described by Vedenov and Ryutov (1975) using a one dimensional approximation, where the magnetic field is parallel to the beam velocity, and is strong enough to suppress oscillations that propagate at an angle to the beam axis. They show that for an initial beam velocity, v_o, background density, n, and beam density, n', the relaxation length is given by,

$$l_{1/2} = .2\frac{n}{n'}\frac{v_{Te}^2\Lambda}{\omega_{pe}v_o} \tag{3.9}$$

Where Λ is the Coulomb logarithm, n is the background density and n' is the beam density. A derivation of this parameter is located in the Appendix.

Vedenov and Ryutov [1975] also describe a relaxation wave which is caused by an electron beam when the plasma is heated by the beam itself, as is the case in VTF. When the beam turns on there will be positive energy in a layer of thickness $z \sim l_{\frac{1}{2}}$. The plasma initially formed will then expand with a high velocity and become more inhomogeneous. As the density in this layer increases, the density gradient reaches a critical value, corresponding to a break in the instability, and the energy starts to be generated in the next layer, again with thickness $\sim l_{\frac{1}{2}}$. This region of relaxation propagates into the plasma. For narrow beam paths, and small thermal conductivity and electron mean free path, Vedenov and Ryutov (1975) show that the velocity of this relaxation wave is $v \sim \sqrt{\frac{T}{M}}\frac{l_{\frac{1}{2}}}{a}\sqrt{\frac{L_{\|crit}}{l_{\frac{1}{2}}}}$ which is much greater than the acoustic velocity in the plasma.

3.3 Comparison With Other Laboratory Experiments

Laboratory experiments have been conducted by Kellogg et. al. (1986) in a vacuum chamber with the electron beam parallel to the magnetic field. The neutral pressure and magnetic field strength approximated the ionospheric E-region. The waves that were measured can be summarized into three categories: A low frequency spectrum with $f \ll f_{ce}, f_p$, a whistler mode spectrum extending up to f_{ce}, and a high frequency range near f_{pe}. The low frequency waves were attributed to surface waves and a lower hybrid drift instability. The whistler mode is most likely due to a Cerenkov resonance with the lower Trivelpiece-Gould mode. The high frequency waves are believed to be due to a Cerenkov resonance with the upper Trivelpiece-Gould mode, with peaks separated by the Langmuir-Bernstein spectrum. An antenna system was configured using two ropes suspending an antenna which could be moved anywhere on a plane within the chamber.

In the earliest rocket experiment to measure waves from electron beams, Electron Echo [Kellogg, et. al., 1986], the waves were strong in the first few milliseconds after the electron gun was turned on, but disappeared well before the end of the gun pulse. This effect in Echo I and ARAKS has been attributed to radiation due to the sharp turnon of the electron beam. But in Echo I it took more time to reach full voltage, so the turnon was not very sharp, but the enhancement during the first few milliseconds was still present. In the beam chamber experiments conducted by Kellogg, et. al. (1986), the initial strong waves lasted a few milliseconds, while the beam only takes 1 μs to travel the length of the chamber. Therefore, it is presumed that the initial radiation and sharp decrease are associated with the plasma density approaching equilibrium.

In the same beam chamber experiments, the electron energy distributions were also measured. According to Jost, et. al., (1980), these distributions were measured with

an electrostatic deflection analyzer. With a low beam current, a sharp peak occurred at the acceleration potential. At high beam currents a beam plasma discharge occurs and the electron energies are redistributed so that the energy peak broadens and a strongly enhanced low energy tail is present. They also found that Langmuir waves are an important part of beam plasma discharge as are lower frequency electric field oscillations.

Chapter 4

Analysis of Results

4.1 Radial Probe Measurements

4.1.1 Plasma Density

The density experiments were conducted for combinations of different plasma sources, namely, Taylor discharge, and one or two electron beams. The density profiles obtained for a Taylor discharge plasma is shown in Figure 4-1. The radial profiles for Taylor discharge plasma in conjunction with one and two electron beams are shown in Figure 4-2 and Figure 4-3, respectively. Note that these density values do not take into account the multiple ionization described in section 2.2. The oscillations in each profile are due to the 1200 Hz of the Taylor discharge circuit. An important observation is that with Taylor discharge, and two electron beams running we achieved a density of $1.26 \cdot 10^{12} cm^{-3}$. Using the formula for f_{pe} and f_{ce} we find that $\frac{f_{pe}}{f_{ce}} = 2.2$ which constitutes an overdense plasma. The resulting ratios and parameters for each set of conditions is shown in Table 4.1.

It is important to note that the peak for the Taylor discharge plasma alone occurs very close to the inner wall. The sinusoidal amplitude of the loop voltage at the midplane of the chamber and the voltage across the 45 coils were both measured. The values obtained are shown in Table 4.2.

Table 4.1: Table of Results From Density Measurements.

	Taylor Discharge	T.D. + 1 beam	T.D. + 2 beams
Peak Density (m^{-3})	$8.5 \cdot 10^{16}$	$3.25 \cdot 10^{17}$	$1.26 \cdot 10^{18}$
TF Current (A)	7300	7300	12000
f_{pe} (GHz)	2.62	5.13	10.1
f_{ce} (GHz)	3.68	3.68	4.56
Peak Radius (cm)	80	80	106
Ratio $\frac{f_{pe}}{f_{ce}}$	.7	1.39	2.2

Table 4.2: Measurements of Loop and Coil Voltage in Taylor Discharge Circuit.

	Loop Voltage (V)	Coil Voltage (V)
Hydrogen	13.6	970
Argon	8.5	670

A minimum breakdown voltage is required to form plasma in the chamber and since the loop voltage is greater near the inner wall it is easier for plasma to form at this radial position. One of the major problems with the current setup is getting enough power coupled to the plasma to achieve a large density. This result also shows that it is hard to combine the Taylor discharge density with the electron beam densities which have peaks occurring at the center of the outer radius. In Figure 4-2 two peaks are easily distinguished, due to Taylor Discharge and the electron beam, respectively. However, in Figure 4-3 the density produced by two electron beams outshadows the Taylor discharge contribution. It is thus possible to produce an overdense plasma by only using electron beams. Once better coupling is achieved through a series supply and iron core, we expect to produce a much greater density with Taylor discharge, thus increasing the ratio of $\frac{f_{pe}}{f_{ce}}$.

4.1.2 Floating Potential

Floating potential profiles were then measured. When only the North Middle beam was used, the peak value was around $-7.5V$. Similarly, with the South Top beam, the peak was around $-8V$. When both beams were being run together, the peak

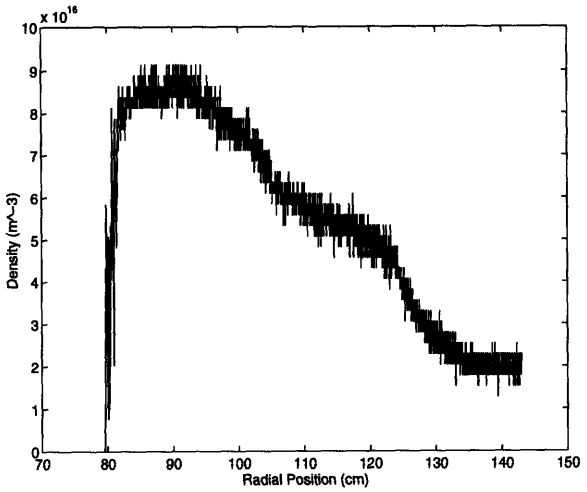

Figure 4-1: Radial Density Profile for a Taylor Discharge Plasma.

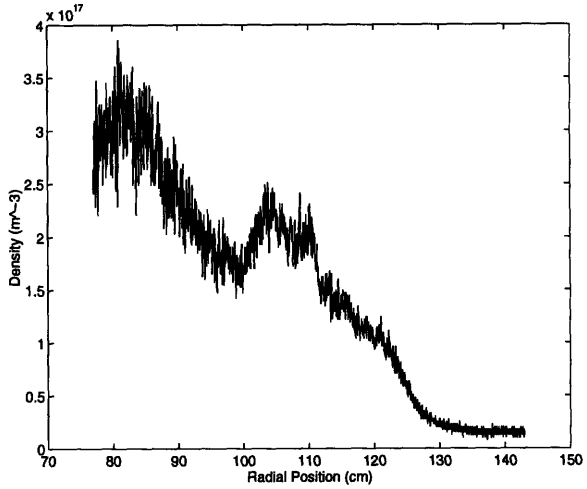

Figure 4-2: Radial Density Profile for Plasma Formed by Taylor Discharge and North Middle Filament.

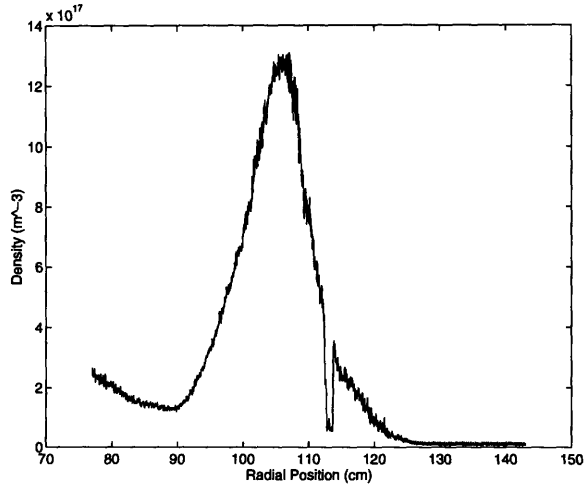

Figure 4-3: Radial Density Profile for Plasma Formed by Taylor Discharge and North Middle and South Top Filaments.

value was -20V. The peak floating potential generally occurred at mid-radius, which corresponds to the position of highest plasma density.

4.1.3 Spectra Measurements

Frequency spectra were measured using the radial probe, while pulsing the North Middle electron beam. The frequency power was measured for six distinct frequencies: 1, 5, 10, 50, 100, and 500 MHz. Eight pulses of 10 ms duration were equally spaced across the 65.1 cm sweep of the probe. It was found that the arc voltage turns on $\approx$ 30 ms after the input signal is sent. Because it is not precisely a 30 ms delay, the spectra data was digitized for 20 ms, within which the arc voltage came on for 10 ms. The timing of each pulse is illustrated in Figure 4-4. In this figure, at 0 ms the PLC sends a command telling the arc voltage to switch on. However, it is not until $\approx$ 30 ms later that the arc voltage physically turns on. A 32768 byte memory module was used to store four signals: Langmuir probe current, arc voltage, and the x and y axes of the power spectrum. Digitizing was done at a rate of 200 KHz. With four channels there is a 40.96 ms digitizing window. Thus we could digitize two pulses during each shot. Four shots were done to get the full radial profile for each frequency.

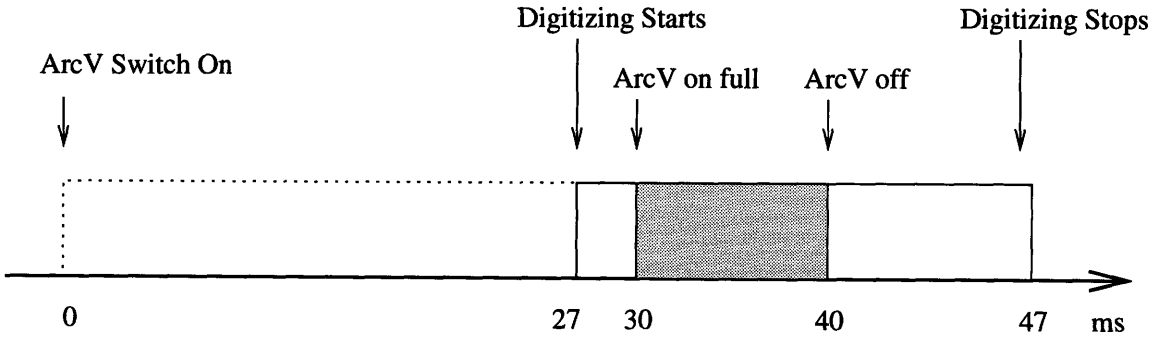

Figure 4-4: Timing of Arc Voltage and Digitizer During Beam Pulse

The spectra for these experiments are shown in Figures 4-5 through 4-10. Only the first 5 ms of the pulse are shown because during the last 5 ms the spectra data stayed relatively constant. The density during these pulses was measured simultaneously, and is shown in Figure 4-11. By comparison with Figure 4-11, it is visible that the

position of maximum power coincides with the highest density. It should be noted that the power values in these graphs are not the true calibrated values. The correct values can be obtained by adding 36 dBm to the measured power level from the spectrum analyzer. For the following analysis, I will refer to the uncalibrated values.

The maximum power level at 1 MHz is -49.8 dBm. The level is a little higher at 5 MHz with a maximum of -46.7 dBm, whereas at 10 MHz the maximum power goes down slightly to -48.4 dBm. The power then increases with maximum values of -45.69 dBm, -40.72 dBm, and -29.53 dBm, occurring at 50 MHz, 100 MHz, and 500 MHz, respectively. Note that each of these peaks occur while the plasma is already in steady state.

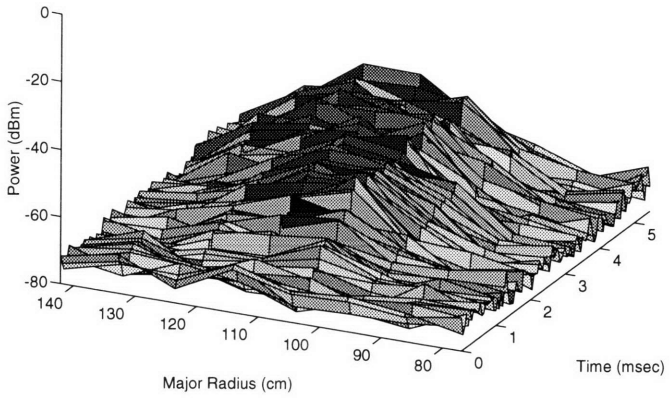

Figure 4-5: Power at 1 MHz Versus Time and Major Radius Measured by the Radial Probe

4.2 Vertical Probe Measurements

4.2.1 Plasma Density

Density measurements were done using the vertical probe on the chamber floor. The probe has a fixed radial position but is able to be moved upward to 47.5 cm

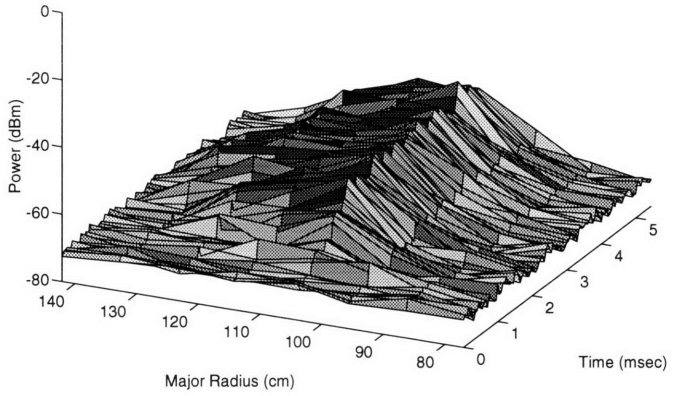

Figure 4-6: Power at 5 MHz Versus Time and Major Radius Measured by the Radial Probe

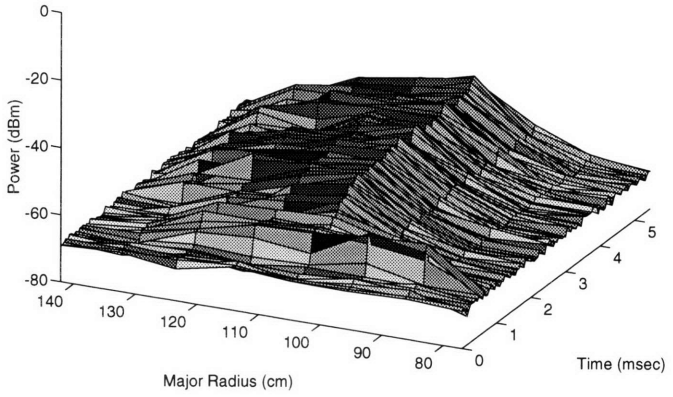

Figure 4-7: Power at 10 MHz Versus Time and Major Radius Measured by the Radial Probe

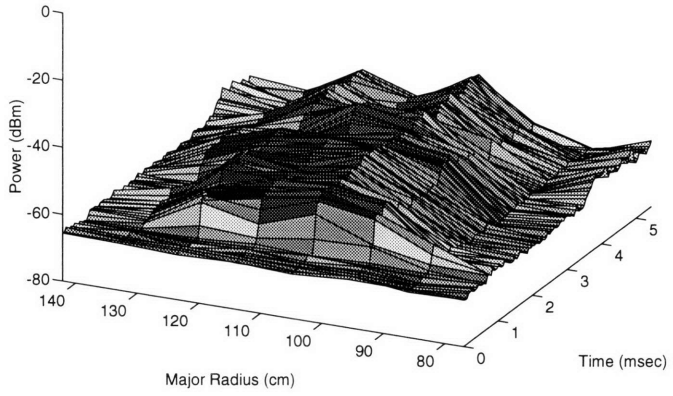

Figure 4-8: Power at 50 MHz Versus Time and Major Radius Measured by the Radial Probe

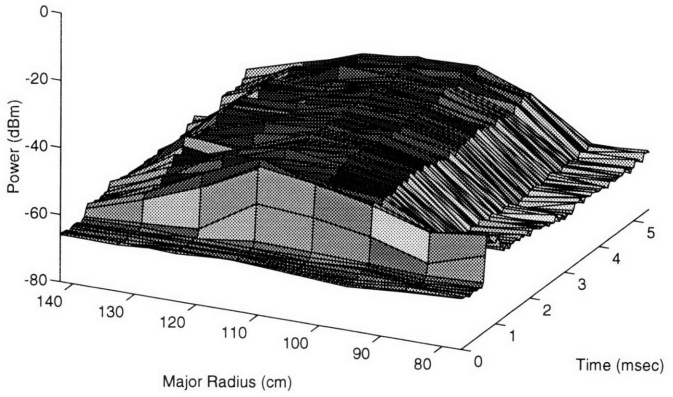

Figure 4-9: Power at 100 MHz Versus Time and Major Radius Measured by the Radial Probe

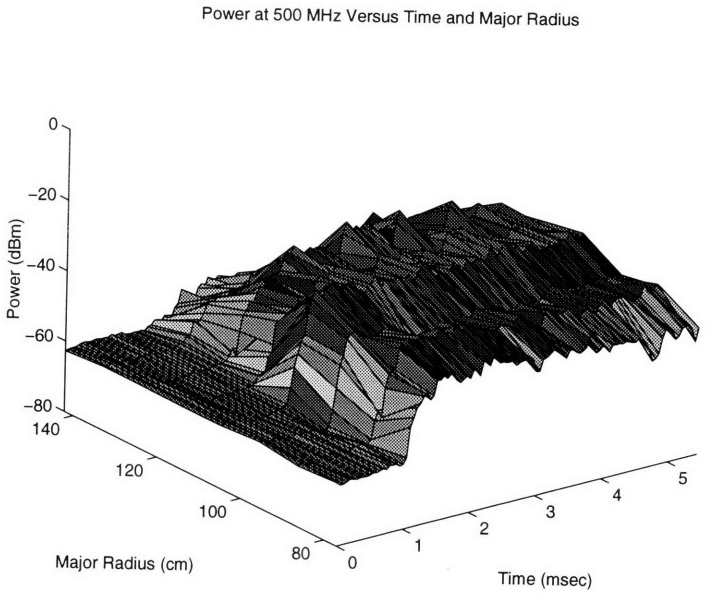

Figure 4-10: Power at 500 MHz Versus Time and Major Radius Measured by the Radial Probe

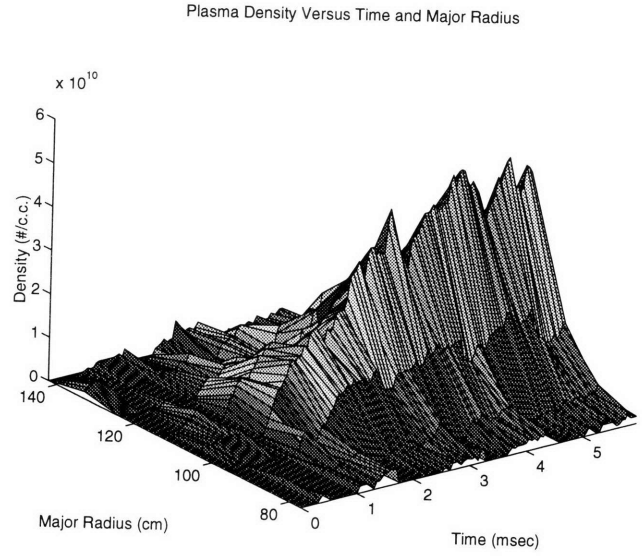

Figure 4-11: Plasma Density Versus Time and Major Radius Measured by the Radial Probe

above the chamber floor. The plasma density at this location near the chamber floor was measured while running the South Top electron beam located 27 cm away. The profiles measured by two different probe tips is shown in Figure 4-12. The last values measured by each tip correspond to the height of the electron beam.

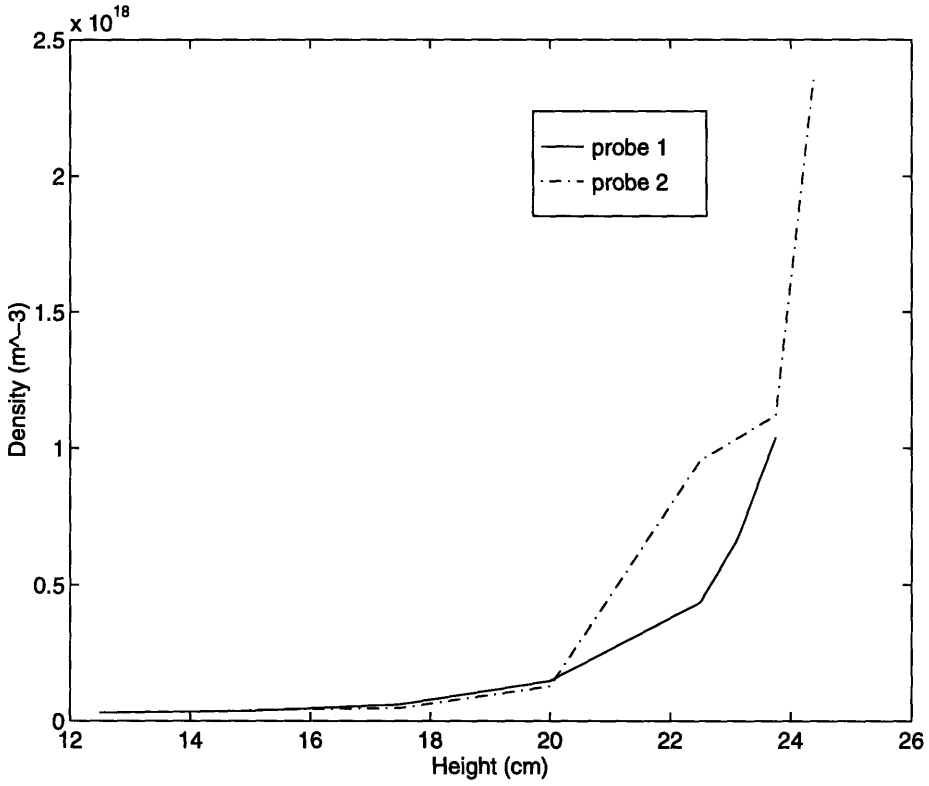

Figure 4-12: Plasma Density Measured by Vertical Probe With South Top Filament On

4.2.2 Floating Potential

The next set of experiments was performed to see how the floating potential changes from the beam to the middle of the beam path at the midplane. The potential profile in the upper half of the chamber was found to drop from -120 V at the midplane to -20 V at the edge of the sheath of the collector plate [Beals, 1994].

The floating potential was measured for combinations of the two electron beams. By using only beam-generated plasma, we can study how well our electron beams emulate the electron guns used on the space shuttle. These measurements will aid

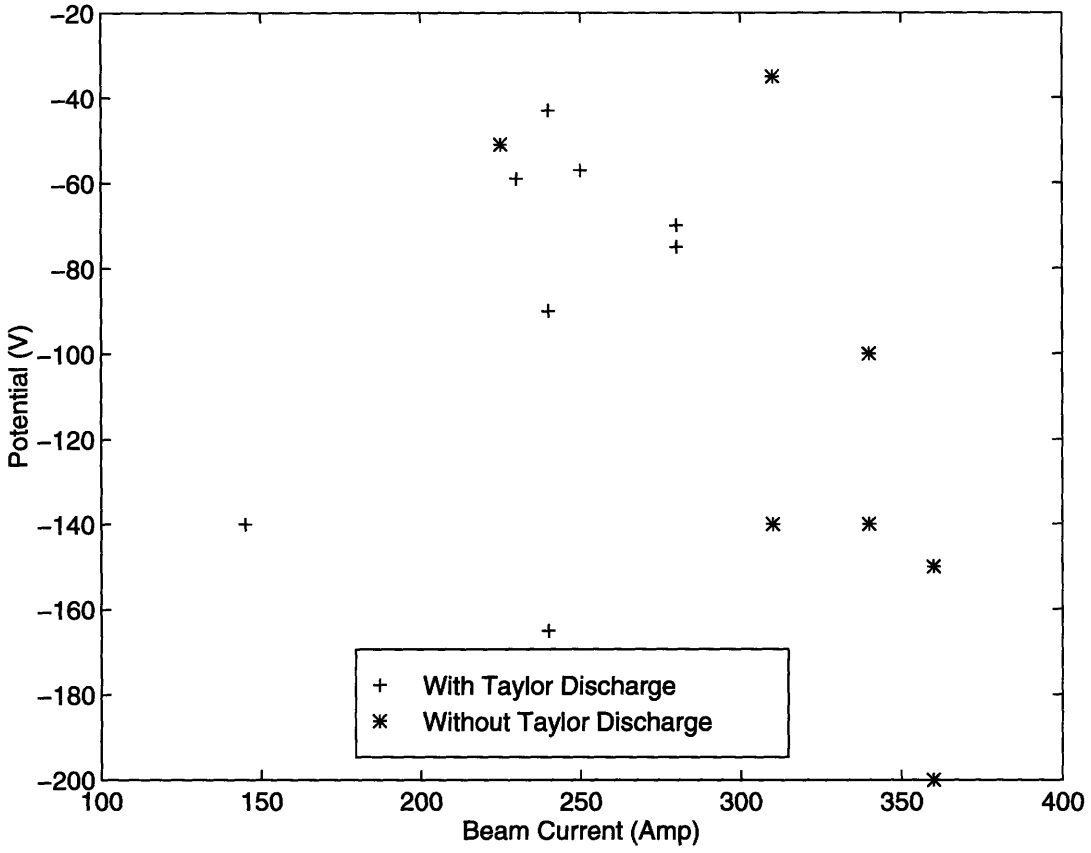

Figure 4-13: Scatterplot of Floating Potential Measured by Vertical Probe and Total Current From Two Beams.

in determining the energy distribution of beam electrons in the VTF. The energy distribution will be very useful in determining what types of instabilities can exist in the VTF.

As illustrated in Figure 4-13, there is a lot of spread in the data. The current emitted from each of the filaments is set to regulate at $200A$, but this level of current is rarely achieved. When running one beam at a time, the current usually stays below $50A$. When two beams are being run, the current out of each tends to be between 150 and 200 A. Figure 4-13 also demonstrates that more beam current is generally achieved in the absence of Taylor Discharge. One reason for this is that the $\sim$ 1 kHz oscillation in the Taylor discharge circuit causes aliasing in the measured beam current, which is digitized at 200 Hz. This oscillation may be limiting the amount of beam current being emitted as shown in Figure 4-14.

4.2.3 Spectra Measurements

Using the vertical probe, the spectra was measured from 10 MHz to 10 GHz for Taylor discharge plasma, with and without electron beams, however, no prominent peaks or enhancements were detected. Close to the beam, we hypothesize that waves have not had time to grow or cause instabilities, since the electrons are just starting to accelerate at this point. If a true electron gun were used in the VTF, we would expect to see wave activity around f_{ce} as well as lower hybrid instabilities which can occur with the existence of tail electrons in the energy distribution.

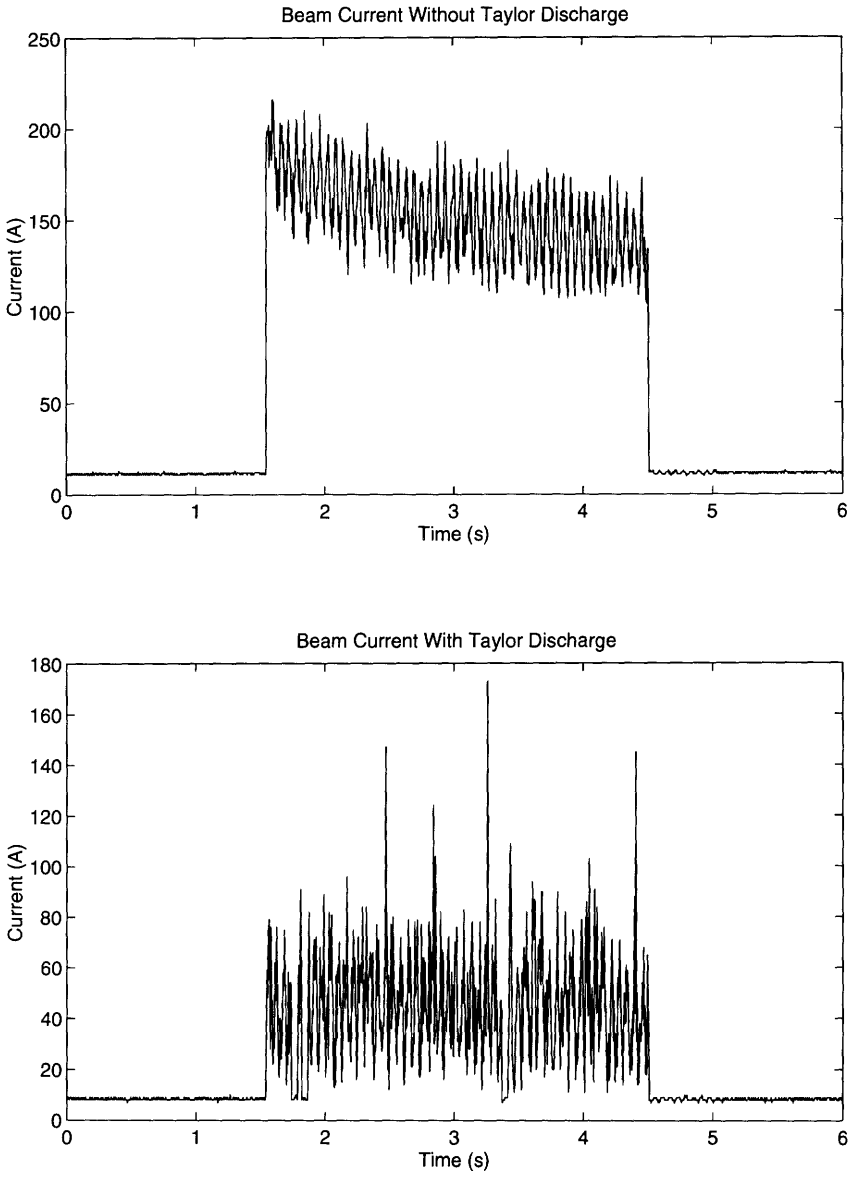

Figure 4-14: Current From South Top Filament With and Without Taylor Discharge Running.

Chapter 5

Conclusions

5.1 Summary of Results

The results of this work help to characterize the plasma properties in the vicinity of the beam and how these properties differ at different locations within the chamber. The Taylor discharge unit in its current configuration was not able to produce an overdense plasma alone. Modifications to the circuitry should be explored and implemented to insure that more of the power goes into the plasma.

The current being emitted by each filament varies a lot from shot to shot. It seems to depend on the pressure, the number of beams being run together, as well as how recently the vacuum had been broken. This last item is important because when the vessel is brought up to atmospheric pressure, many impurities settle on the filaments and the chamber walls. This accumulation reduces the amount of emitted current that is achieved until the impurities have been heated off.

5.2 Limitations of the Current Configuration

The current setup and diagnostics of the VTF pose certain constraints in determining how well the shuttle experiments can be simulated. The LaB_6 filaments are able to provide an overdense plasma, however without an electron gun it is more difficult

to achieve an energy distribution with high energy tail electrons.

Pulsing of the beams is limited by the turn on time of the arc voltage as well as the delay of the arc current turning on, as illustrated in Figure 5-1. Aside from the initial 30 ms arc voltage switch delay, it takes $\approx$ 100 μs for the arc voltage to rise to its full value once the supply has been physically turned on. The arc current then turns on between 2 and 5 ms later. This delay makes it difficult to run shorter pulses because there might not be enough time for the arc current to come on and for the plasma to be formed.

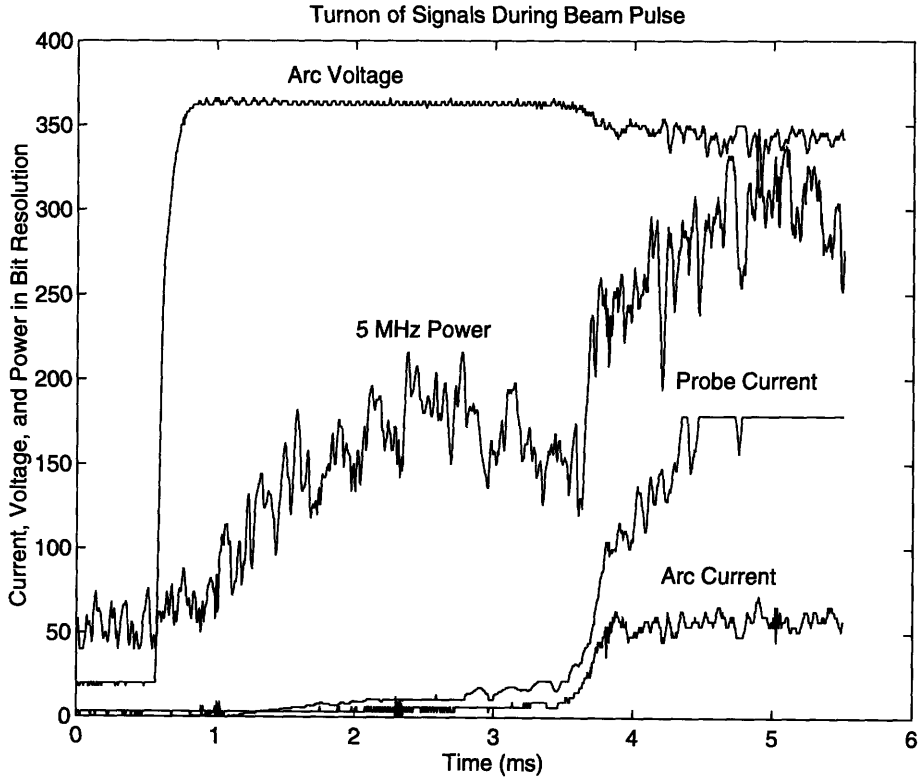

Figure 5-1: Graph Showing the Turnon of Arc Voltage, Arc Current, Probe Current, and 5 MHz Power at the Beginning of a Beam Pulse.

The probe measurements are also limited in how much of the chamber is scannable. The existing side probe can make a radial scan along the midplane of the chamber. There also exists a top vertical probe which can make measurements in the top half of the chamber along mid-radius. The vertical probe on the bottom which was recently

installed can move up to 47.5 cm above the chamber floor, also at mid-radius.

5.3 Future Work for Ionospheric Simulation

Because of the constraints on producing a plasma environment analogous to that produced by the FPEGs it would be beneficial to install an electron gun at the bottom of the chamber and to place the vertical probe close enough to detect the tail electrons in the velocity distribution. An overdense background plasma can be provided by the Taylor discharge method together with 2 or 3 other beams, or Taylor discharge by itself with an iron core added to replace the present air core. The electron gun should then be pulsed at the same rate as the FPEGs.

An energy analyzer similar to the ESAs of the shuttle experiments, would also provide valuable measurements. Then the energy distribution could be measured close to the electron gun and also at the side probe. The effects of changing the beam current could then be studied and compared with the results of Vedenov and Ryutov (1975).

Another valuable addition would be an array of mobile probes either vertical or radial. This type of array would allow us to obtain a two-dimensional density profile like the one obtained by Kellogg, et. al. [10].

In summary, the VTF is suitable for simulating ionospheric plasma. Overdense plasma conditions have been achieved with $\frac{f_{pe}}{f_{ce}} = 2.2$. Installing precise electron guns would provide more control and flexibility in the beam pulses and consequently a more accurate representation of the active experiments conducted in space.

Bibliography

[1] Beals, Dexter F. *Characterization of a Hot Cathode Helimak Plasma,* Masters Thesis, MIT, 1994.

[2] Cartwright, D. C. and P. J. Kellogg. *Observations of Radiation From an Electron Beam Artificially Injected into the Ionosphere,* Journal of Geophysical Research, Vol. 79, 1974.

[3] Chen, F. F. *Introduction to Plasma Physics,* Plenum, New York, 1977.

[4] Dobrowolny, M. *Il Nuovo Cimento,* Societa Italiana di Fisica, Vol. 17C, N. 1, 1994.

[5] Gewartowski, J. W. and H. A. Watson. *Principles of Electron Tubes,* D. Van Nostrand Company, Inc., Princeton, NJ, 1965.

[6] Gough, M. Paul, David A. Hardy, Marilyn R. Oberhardt, William J. Burke, Louise C. Gentile. *Correlator Measurements of MHz Wave-Particle Interactions During TSS 1 Electron Beam Operations,* U.S. Air Force Office of Scientific Research, 1995.

[7] Hardy, David A., Marilyn R. Oberhardt, William J. Burke, Donald C. Thompson, W. John Raitt, Louise C. Gentile. *Electron Beam Propagation Observed During TSS 1,* U.S. Air Force Office of Scientific Research, 1995.

[8] Hutchinson, Ian. *Principles of Plasma Diagnostics,* Cambridge University Press, Cambridge, 1987.

[9] Jost, R. J., H. R. Anderson, and J. O. McGarity. *Electron Energy Distributions Measured During Electron Beam/Plasma Interactions,* Geophysical Research Letters, Vol. 7, No. 7, July 1980.

[10] Kellogg, Paul J., Steven J. Monson, Robert H. Holzworth, and R. Jerry Jost. *Beam-Generated Waves in a Large Plasma Chamber,* IEEE Transactions on Plasma Science, Vol. PS-14, No. 6, December 1986.

[11] Spangenberg, Karl R. *Vacuum Tubes,* First Edition, McGraw-Hill, New York, 1948.

[12] Vedenov, A. A. and D. D. Ryutov. *Quasilinear Effects in Two-Stream Instabilities,* Reviews of Plasma Physics, Vol. 6, 1975.

[13] Walker, D. N. and E. P. Szuszczewicz. *Electrostatic Wave Observation During a Space Simulation Beam-Plasma Discharge,* Journal of Geophysical Research, Vol. 90, 1985.

Appendix

Derivation of Relaxation Length

Vedenov and Ryutov (1975) derive the beam relaxation length using a one-dimensional model which is appropriate when an electron beam is traveling parallel to the magnetic field and when this field is strong enough to suppress oscillations propagating obliquely to the beam axis. The spectral function, $W(k_z, t)$, is also one-dimensional. The Cerenkov resonance condition for this situation is $\omega_{pe} - k_z v_z = 0$.

Assuming that the electrons in the ambient plasma are described by a maxwellian distribution, $F = \frac{n}{\sqrt{2\pi} v_{Te}} exp\,(-\frac{v_z^2}{2v_{Te}^2})$, and the beam component is narrow enough to approximate it as:

$$f - \frac{2\omega_{pe}}{m} \cdot \frac{d}{dv_z} \cdot \frac{W}{v_z^3} = f_\circ = n' \delta(v_z - v_\circ) \tag{5.1}$$

Assuming that the initial beam spread is $\Delta v_\circ$, and the final beam spread is Δv then $\Delta v_\circ \ll \Delta v$. The ratio of these spreads become:

$$\frac{\Delta v}{v_\circ} \leq (\frac{n'}{n})^{\frac{1}{3}} \tag{5.2}$$

The velocity distribution at this peak, $f(v_\circ)$, can only spread toward lower velocities, and $f_\infty = const$ in the stationary state to which the beam relaxes. $f_\infty = 0$ for $v > v_\circ$ and $f_\infty = \frac{n'}{v_\circ}$ for $0 < v < v_\circ$.

It follows that the lower limit of this plateau is a velocity $v_z = v_{min}$ at which point the value along the plateau is equal to the electron distribution in the background plasma where,

$$v_{min} = v_{Te} \sqrt{2ln(\frac{n}{n'} \cdot \frac{v_\circ}{v_{Te}})} \tag{5.3}$$

One third of the initial energy is in the final distribution, whereas the other two thirds go into plasma oscillations. The minimum velocity of the plateau distribution is defined as: The ratio of the energy of thermal fluctuations to thermal energy is $\frac{U_T}{nT_e} \sim N_D^{-1}$ where $N_D = n\frac{4}{3}\pi(\frac{v_{Te}}{\omega_{pe}})^3$ which is the number of particles in a Debye sphere.

We need to determine how far away from the beam we can place the probe and still measure the high energy electrons.

The time at which electrons from the beam are left with an energy of $\frac{mn_o'^2}{3}$ is defined to be:

$$t_{\frac{1}{2}} = \frac{\Lambda}{\pi\omega_{pe}} \cdot \frac{n}{n'}(\frac{\sqrt{5}-1}{2} + ln(\frac{\sqrt{5}-1}{2})) \tag{5.4}$$

$$\simeq .07\frac{\Lambda}{\omega_{pe}} \cdot \frac{n}{n'} \tag{5.5}$$

$$\Lambda = ln\frac{\tilde{U}_{\inf}}{\tilde{U}_T} \tag{5.6}$$

During the relaxation process, the distribution function keeps the form of a step with:

$$f = \frac{2n_o'v_o}{v_o^2 - u^2},\ u < v_z < v_o \tag{5.7}$$

$$f = 0,\ v_z < u \tag{5.8}$$

where the function u(z) is given by:

$$\frac{v_o^2 - u^2}{2u^2} - ln\frac{v_o}{u} = \frac{2\pi}{3} \cdot \frac{n_o'}{n} \cdot \frac{\omega_{pe}v_o z}{\Lambda v_{Te}^2} \tag{5.9}$$

The beam loses an energy density of $\frac{mn_o'v_o^2}{12}$ in a distance:

$$l_{\frac{1}{2}} = 0.2\frac{n}{n'} \cdot \frac{v_{Te}^2}{\omega_{pe}v_o}\Lambda \tag{5.10}$$